Journal of Applied Sciences

ISSN 1812-5654

Journal of Applied Sciences 8 (6): 975-983, 2008
ISSN 1812-5654

Developing Seismic Fragility Function of Structures by Stochastic Approach

K. Nasserasadi, M. Ghafory-Ashtiany, S. Eshghi and M.R. Zolfaghari
International Institute of Earthquake Engineering and Seismology,
P.O. Box 19395-3913, Tehran, Iran

Abstract: Fragility function of structures is the major requirement of seismic loss estimation which is widely used in the seismic risk management. In this study, a comprehensive and simplifies stochastic methods are presented and the effect of damage threshold uncertainty on fragility functions is estimated. The method is employed to estimate the fragility of low-rise steel moment framed structure. It is shown that the results of the method are almost comparable with the result of previous studies and the effect of uncertainty of damage state on the deviation of fragility function in the lower intensity of ground motion is high. The deviation then gradually decreases.

Key words: Fragility function, fragility dispersion, steel structure, HAZUS, vulnerability

INTRODUCTION

Evaluation of seismic fragility functions of structures which defines the probability of physical damage as a function of ground motion intensity parameter has gained importance recently due to its key role in seismic loss assessment and risk management. Although some well-known fragility databases such as ATC (1985) and Hazus (1999) are available, these fragility functions are developed for general types of structures with substantial amount of assumptions and uncertainties. Due to wide usage of fragility functions in the next generation of seismic design codes (Porter *et al*., 2007), need for development of structure-specific fragility functions has increased. As an answer to such demand, in this study, a comprehensive stochastic method with a proposed simplified procedure is introduced. From the fragility's uncertainty point of view, few studied has been conducted. In the recent one, Kwon and Elnashai (2006) studied the effect of uncertainty of material and ground motion on the fragility function and has shown that the ground motion randomness have more effect on the fragility function. Among other factors which affect the uncertainty of the fragility, the uncertainties of damage threshold which describe the physical state of structure have not been investigated. In this study, this effect has been studies by a proposed methodology.

Fragility and vulnerability functions are developed by three main ways: expert opinion, analytical methods and damage data of structures from past events (Porter *et al*., 2007). Evaluation of fragility curves using existing data of earthquake damage is perhaps the best way to estimate potential damage of future earthquake and has been used for fragility functions development in several studies such as the work which have done by O'Rourke and So (2000), Sabbetta *et al*. (1998), Shinozoka *et al*. (2000a) and Sarabandari *et al*. (2004). In the absence of past damage data, the fragility functions are developed based on the opinion of experts. ATC (1985) is a good example of such approach. Nevertheless, when appropriate analytical tools are available, the analytical method is the proper method for fragility curve development of engineering and special structures.

Two general approaches have been utilized for development of analytical fragility functions: comparing capacity and demand of structures (Dimova and Hirata, 2000; Shinozoka *et al*., 2000a, b) and employing damage index (Hwang and Huo, 1994; Karim and Yamazaki, 2001, 2003; Smyth *et al*., 2004). Results of the first approach are more suitable for design purposes (Bazzurro *et al*., 2004) while the results of the second methodology are more appropriate for the loss estimation purposes due to its ability to define damage states.

Stochastic methods by the means of Monte-Carlo simulation and artificial earthquake records generation have been employed for fragility functions (Hwang and Huo, 1994; Karim and Yamazaki, 2001, 2003; Singhal and Kiremidjian, 1996). However, due to existing uncertainties in these methods, demand for a straight-forward and rapid procedure of structure-specific fragility function calculation is still existed.

Corresponding Author: K. Nasserasadi, International Institute of Earthquake Engineering and Seismology, No. 26 Arghavan St. North Dibaji Av. P.O. Box 19395-3913, Tehran, Iran
Tel: +98 21 2283116-19/376, +98 912 1077881 Fax: +98 21 88044423

The main objective of this study is demonstrating the procedure of structural fragility function development in a clear and transparent manner and presenting a simple methodology for structure-specific fragility function derivation. Besides, some challenging issues such as effect of damage threshold uncertainty on fragility dispersion and fragility function of structures with non-structural governing damage cases which is used for industrial facilities are discussed.

DEFINITION OF FRAGILITY FUNCTION AND ESTIMATION METHOD

Due to practical reasons, continuous damage in structures is divided into several discrete damage states (Porter, 2000). Fragility function estimates the conditional exceeding probability of damage from a damage state at given ground motion intensity:

$$F_i(im) = P(D > d_i \mid IM = im) \tag{1}$$

where, F_i (im) is the probability of exceeding damage D from damage state d_i at given ground motion IM = im. Ground motion intensity parameter denotes the magnitude of ground motion which is measured by Peak Ground Acceleration (PGA), Peak Ground Velocity (PGV) or Spectral Displacement (SD). Damage states i are defined from the non-damage state (i = 0) to the nth damage state (i = n) by qualitative and analytical definitions (Porter, 2000). Since damage in structures is measured by Damage Index (DI), Eq. 1 is changed to:

$$F_i(im) = P(DI > di_t \mid IM = im) \tag{2}$$

where, di_t is the damage index at the threshold of damage states. Having the Probability Density Function of DI or its cumulative distribution function at every im (f_{im} (di) and $F_{im}(di_t)$), Eq. 2 is evaluated from probabilistic theorem:

$$F_t(im) = P(DI > di_t \mid IM = im) = 1 - F_{im}(di_t) = 1 - \int_{-\infty}^{di_t} f_{im}(di)d(di) \tag{3}$$

In this study, PDF of DI is evaluated by multi-stripe analysis used by Jalayer (2003) and Aslani and Miranda (2004). In this method, structure is analyzed subjected to several real ground motion records that are all scaled to specific IM level and distribution of structural response in the particular IM is estimated from the results of the nonlinear analysis set.

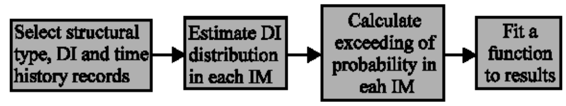

Fig. 1: Procedure of estimating analytical fragility function

Based on these assumptions, procedure of fragility curve development for real structure(s) is summarized in five major steps shown in flowchart of methodology given in Fig. 1:

- Selecting structure(s) with similar structural category and/or behavior
- Choosing a damage index and ground motion intensity measurement
- Selecting group of time history records and scaling them to selected IMs values. The selected records should represent the randomness of ground motion
- Estimating the distribution of damage index at the selected IMs through multi-stripe analyses and fitting proper distribution function to the results
- Calculating fragility values using Eq. 3 and fitting appropriate function to the results.

Implementation of the above procedure is illustrated in the following example.

ILLUSTRATIVE EXAMPLE

Two groups of low-rise steel frame which are compatible with high-code and moderate-code structural classifications of HAZUS were selected (Hazus, 1999). According to HAZUS, high-code frame corresponds to ductile steel structures designed for 0.133 fraction of building weight and moderate-code frame corresponds to semi-ductile steel frames which is designed for 0.067 fraction of building weight. For each classification, two low-rise steel moment resisting frames (two bay; two and three story) which are selected from a middle frame in a hypothetical building were designed. The elevation views of the frames are shown in Fig. 2.

Following assumptions are made for fragility curve development:

- Spectral Displacement (SD) is chosen as IM
- ISD is selected for damage index, due to its good representation of damage for structural and most of non-structural elements (Porter, 2000)
- Mean damage thresholds of HAZUS shown in Table 1 are chosen as medium threshold of damage states (Hazus, 1999)

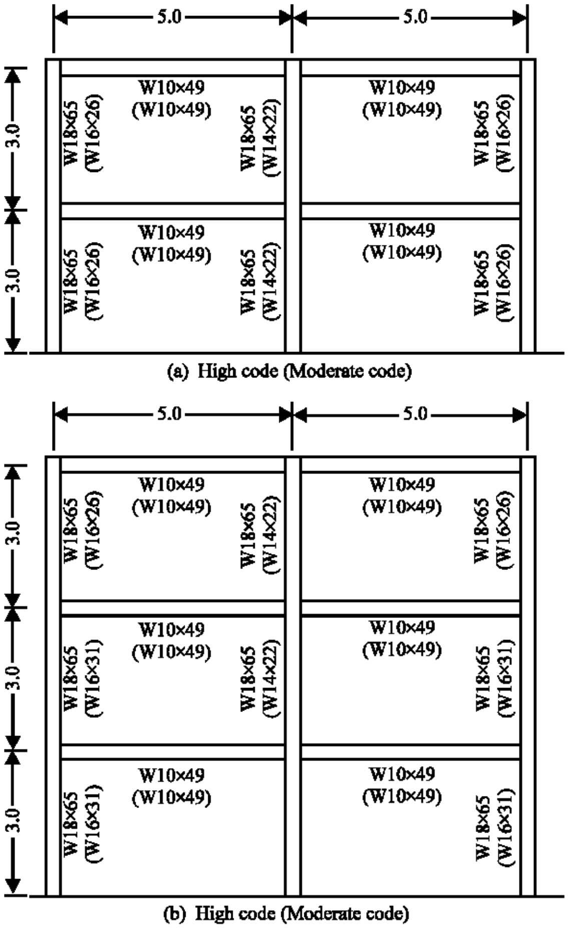

Fig. 2: Elevation of frames selected for analysis; moderate code is in parentheses (a) two story frames and (b) three story frames

For the evaluation of ISD distribution in each ground motion value, a set of 20 records with a uniform distribution of source-to-site at a minimum distance of 10 km to reduce the near source effect were selected from the PEER (2007) ground motion database (Table 2). The distribution of source-to-site distance with the magnitude of selected records is shown in Fig. 3. The records are scaled so that the 5% damped Spectral Displacement of records at the period of structures (0.13 and 0.149 for moderate and high code) equals to 2.5, 5, 10, 20, 30, 40, 50, 60, 70, 80 and 90 cm. Structures were analyzed by OpenSees (2006) subjected to scaled records. P-Δ effect was considered and FEMA-356 force-deformation relationship (FEMA-356, 2000) was selected for the plastic hinge property of the structural elements.

The distribution of maximum ISD which is estimated from the analyses of moderate and high code structures are shown in Fig. 4, 5 where the mean thresholds of

Table 1: Inter-story drift ration at thresholds of different damages states (Hazus, 1999)

Seismic design level	Drift ration at threshold of structural damages: Slight	Moderate	Extensive	Complete
High-code	0.006	0.012	0.03	0.08
Moderate-code	0.006	0.0104	0.0235	0.06

Table 2: Selected strong motion records for non-linear dynamic analysis (PEER, 2007)

ID	EQ name	Date and time of earthquake	Epicenter distance	M
1	Loma Prieta	1989/10/18 00:05	11.20	6.9
2	Anza (Horse Cany)	1980/02/25 10:47	13.00	4.9
3	Kocaeli, Turkey	1999/08/17	17.00	7.4
4	Morgan Hill	1984/04/24 21:15	16.20	6.2
5	Whittier Narrows	1987/10/04 10:59	20.40	5.3
6	Northridge	1994/01/17 12:31	22.70	6.7
7	Loma Prieta	1989/10/18 00:05	30.60	6.9
8	Northridge	1994/01/17 12:31	26.80	6.7
9	Duzce, Turkey	1999/11/12	30.20	7.1
10	Chi-Chi, Taiwan	1999/09/20	42.70	7.6
11	Northridge	1994/01/17 12:31	36.10	6.7
12	Northridge	1994/01/17 12:31	41.70	6.7
13	Landers	1992/06/28 11:58	42.20	7.3
14	Loma Prieta	1989/10/18 00:05	44.80	6.9
15	Northridge	1994/01/17 12:31	47.30	6.7
16	Northridge	1994/01/17 12:31	46.90	6.7
17	Chi-Chi, Taiwan	1999/09/20	57.06	7.6
18	Landers	1992/06/28 11:58	51.70	7.3
19	Chi-Chi, Taiwan	1999/09/20	58.80	7.6
20	Chi-Chi, Taiwan	1999/09/20	59.26	7.6

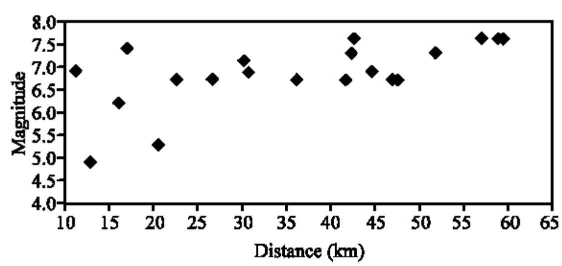

Fig. 3: Distribution of distance and magnitude of selected records

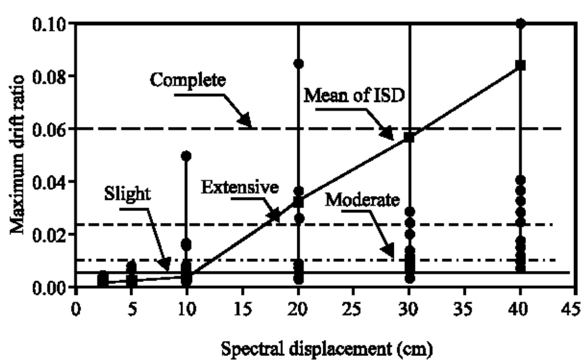

Fig. 4: Maximum ISD of moderate code design frames; horizontal lines are damage thresholds

Table 3: Mean and deviation values of log-normal distribution of ISD data in each SD for high code frame

SD (cm)	2.5	5	10	20	30	40	50	60	70	80	90
$\hat{ISD}_{sd}$	0.001	0.001	0.003	0.005	0.008	0.013	0.018	0.020	0.106	0.139	0.185
β_{sd}	0.778	0.771	0.682	0.702	0.853	1.062	1.106	1.192	1.281	0.973	1.561

Table 4: Parameters of fragility functions estimated from comprehensive procedure

	Slight		Moderate		Extensive		Complete	
Code design level	SD_m (cm)	β	SD_m (cm)	β	SD_m (cm)	β	SD_m (cm)	β
Moderate code	11	0.62	16	0.42	20	0.50	30.12	0.67
High code	26	0.57	37	0.52	55	0.33	69.00	0.35

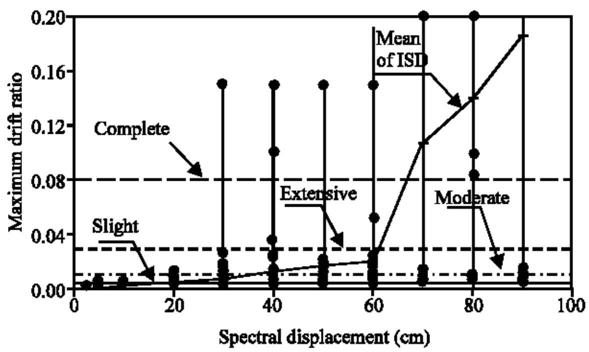

Fig. 5: Maximum ISD of high code design frames; horizontal lines are damage thresholds

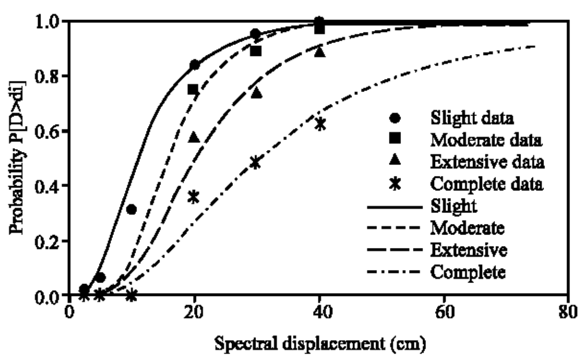

Fig. 6: Fragility values and functions for moderated code design steel moment resistant frame

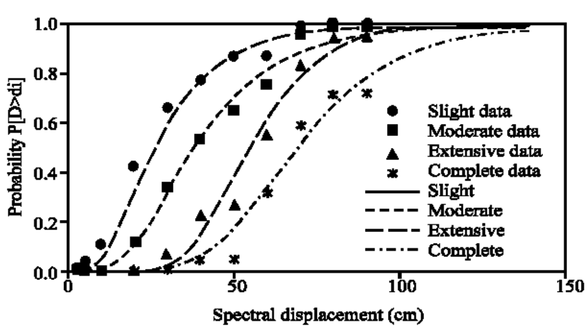

Fig. 7: Fragility values and functions for high code design steel moment resistant frame

damage states from Table 1 are shown as well. To find appropriate distribution function for ISDs, normal and log-normal distribution functions were tested. Even though lognormal distribution rather inappropriate for higher level of SDs especially in the moderate code frames, it is generally better fitted to ISD distributions in general. Mean and lognormal deviation ($\hat{ISD}_{sd}$ and β_{sd}) of ISD distributions of high-code frames are shown in Table 3.

The fragility value at each sd ($F_i(sd)$) is estimated by changing the notation of Eq. 3 and replacing the distribution of damage index ($f_{im}(di)$) by lognormal distribution of ISD ($f(isd) = \phi[\ln(\hat{ISD}_{sd}), \beta_{sd}]$):

$$F_i(sd) = P(D > d_i \mid SD = sd) = 1 - P(D \le d_i \mid SD = sd) = 1 - \Phi(1/\beta_{sd}.\ln(ISD_i/\hat{ISD}_{sd})) \quad (4)$$

where, ISD_i is the mean ISD threshold of damage states (Table 1). The results for the moderate and high code frames are shown in Fig. 6, 7 by dots. Fragility functions shown in the figures are estimated by fitting a log-normal cumulative distribution function:

$$F_i(sd) = P(D > d_i \mid SD = sd) = \Phi(\frac{1}{\beta_i}\ln(\frac{sd}{SD_i})) \quad (5)$$

where, SD_i and β_i are mean and deviation of the function, respectively. These parameters for the fragility functions are shown in Table 4.

Non-structural damage governing case: Most direct and indirect loses stem from the damage to non-structural elements and evaluation of damage probability to these elements is important in the most of the cases. The proposed method provides a useful tool for evaluation of fragility functions when non-structural elements govern the damage states such as supporting structures in industrial facilities. Since the damage to most of the non-structural damages are defined by ISD (Porter, 2000), the relevant fragility function is estimated by replacing the corresponding ISD damage threshold (ISD_i) in Eq. 4.

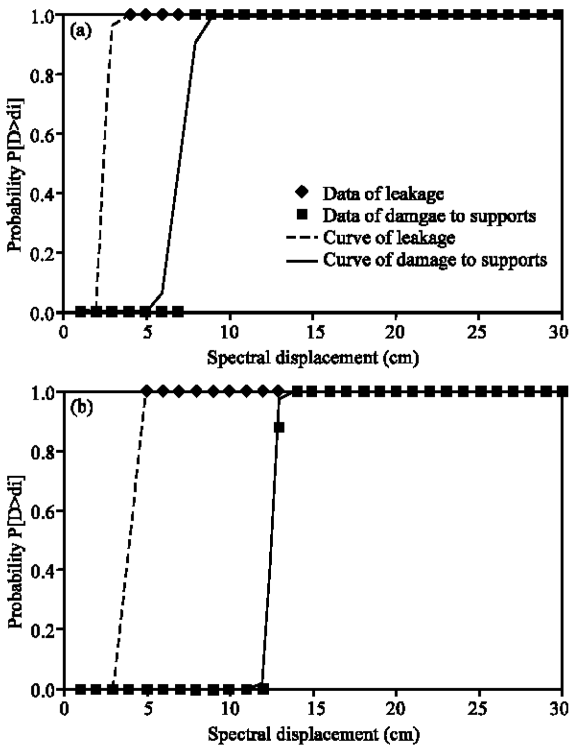

Fig. 8: Fragility function result for equipment governing damage state: probability of leakage in the pipes and damage to equipment support (a) High code and (b) Moderate code

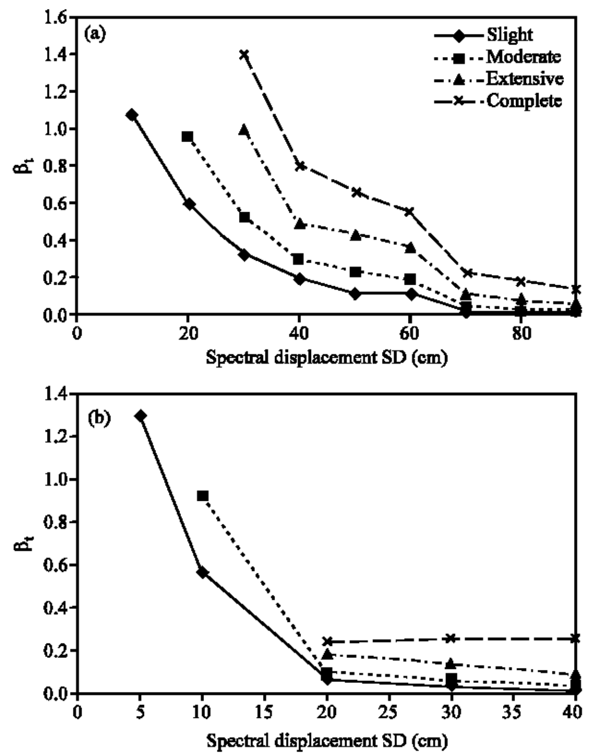

Fig. 9: Deviation of fragility function dispersion (β_t) as a function of SD (a) High code structure and (b) Moderate code structure

These thresholds can be estimated from experimental studies or working condition of equipments.

For instance, in the illustrative example, two additional damage states are defined to determine the pipe leakage and damage to equipment supports with associated ISD of 0.0033 and 0.0083, respectively. The resulted fragility functions which are shown in Fig. 8 can be used to evaluate the probability of relative non-structural damages.

EFFECT OF UNCERTAINTY OF DAMAGE THRESHOLDS

In the current literature, all kind of uncertainties including the uncertainty of damage thresholds are defined by a constant deviation. For example, Kinali and Ellingwood (2007) assumed 0.2 for that. In this stage, the contribution of damage threshold uncertainty on fragility uncertainty is investigated.

Basically, thresholds of damage states, like any other natural phenomena, have statistic nature and are defined by a distribution. According to the existing literature, the lognormal distribution can describe that well (Hazus, 1999; Wen *et al*., 2003):

$$ISD = ISD_i \cdot \varepsilon_{t(i)} \tag{6}$$

where, $\varepsilon_{t(i)}$ is a log-normal distributed random variable with mean of unit and deviation of $\beta_{t(i)}$.

The effect of this uncertainty on fragility functions can be quantified by fragility dispersion. So far, the mean value of fragility function at every ground motion is estimated by using the mean value of damage threshold in Eq. 5 (i.e., ISD_i). By the same token, if the dispersion of damage threshold from Eq. 6 is utilized in Eq. 5, the distribution of fragility value or fragility deviation at every ground motion can be calculated as:

$$F_i(sd) = 1 - \Phi(1/\beta_{sd} \cdot \ln(ISD_i \cdot \varepsilon_{t(i)} / \hat{ISD}_{sd})) \tag{7}$$

Equation 7 has been solved by Monte-Carlos simulation for $\beta_{t(i=1.4)}$, as suggested by Hazus (1999), for all fragility function in the illustrative example and the distribution of fragility value is estimated at every sd. Deviation of fragility function ($\beta_f(sd)$) is estimated by fitting log-normal distribution which is more proper distribution to the fragility distribution at every sd. Figure 9 has shown variation of $\beta_f(sd)$ vs. sd for the fragility functions shown in Fig. 6 and 7.

From Fig. 9 it can be observed that the deviation of fragility function can reach to 3.5 times of damage threshold deviation (i.e., $\beta_{t(i=1.4)} = 0.4$) in the lower IMs and unlike current assumption in the literature, it gradually decreases.

SIMPLIFIED METHOD FOR DEVELOPMENT OF FRAGILITY FUNCTIONS

The proposed method derives the damage index distribution through substantial number of non-linear dynamic analyses which is expensive and inconvenient for most of practical applications. A rapid method of fragility function development is introduced by taking advantage of recent development in estimation of structural capacity by converting push-over (SPO) curve of structures to distribution of incremental dynamic curves (Vamvatsikos and Cornell, 2005) which is very similar to ISD distribution.

The necessary steps for fast derivation of ISD distribution based on flowchart of Fig. 10 are:

- Converting SPO curve of structure from top displacement-base share space to R-μ space by dividing the horizontal axis of the diagram by Δ_y and the vertical axis by V_y
- Generating the set of IDA curves in R-μ space using SPO2IDA software which is available online (Vamvatsikos and Cornell, 2005)
- Converting IDA curves from R-μ space to SD-ISD space by multiplying the horizontal axis by $\theta_{max\,y}$ and vertical axis by $g.S_{ay}/\omega^2$

The simplified method was applied to 3-story structures of the examples shown in Fig. 2. Pushover diagrams of these structures and its converted diagram are shown in Fig. 11. The IDA curve in R-μ space estimated by SPO2IDA software and converted to SD-ISD are shown in Fig. 12. For comparison, the results of non-linear dynamic analyses are shown in the figure as well.

Fragility value at each IM is estimated by applying Eq. 4 to new ISD distribution at each SD. In the Equation, ISD_{sd} is directly estimated from the 50% IDA curve ($x_{50\%}$) and β_{SD} is estimated from and 16 or 84% IDA curves at each IM ($x_{16\%}$ and $x_{84\%}$):

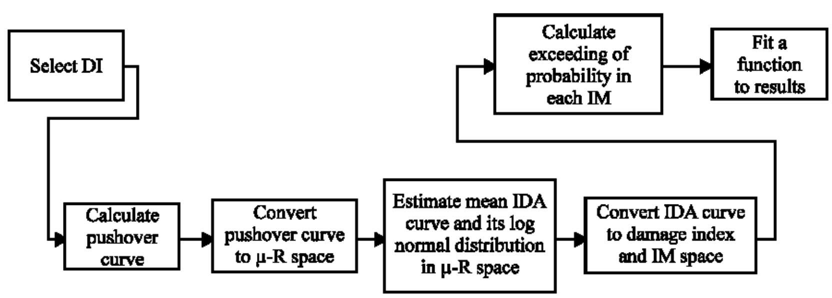

Fig. 10: Flowchart of simplified method of fragility function estimation

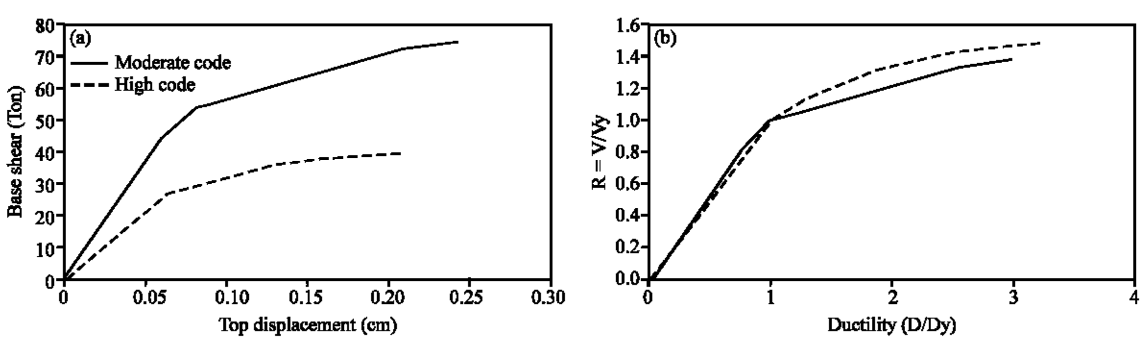

Fig. 11: Pushover curves for high code and moderate code structures (a) Base-shear vs. displacement and (b) Over strength vs. ductility

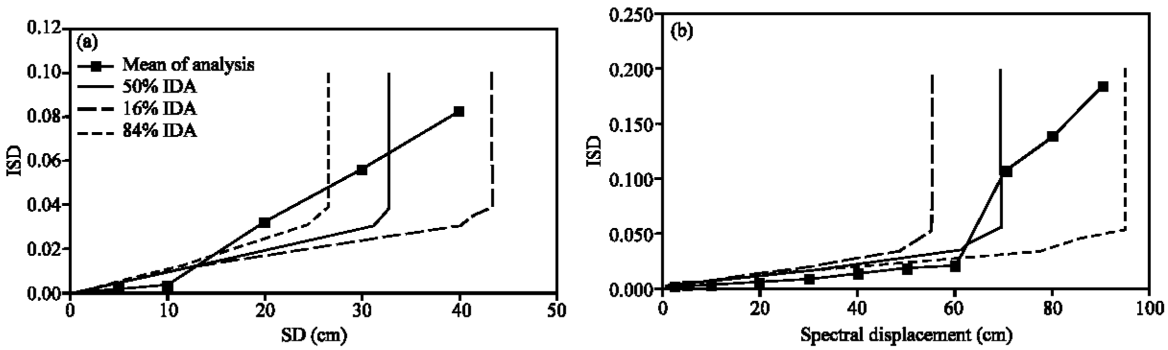

Fig. 12: Converted IDA curve for high code and moderate code structures to SD-ISD space (a) Moderate code IDA and (b) High code IDA

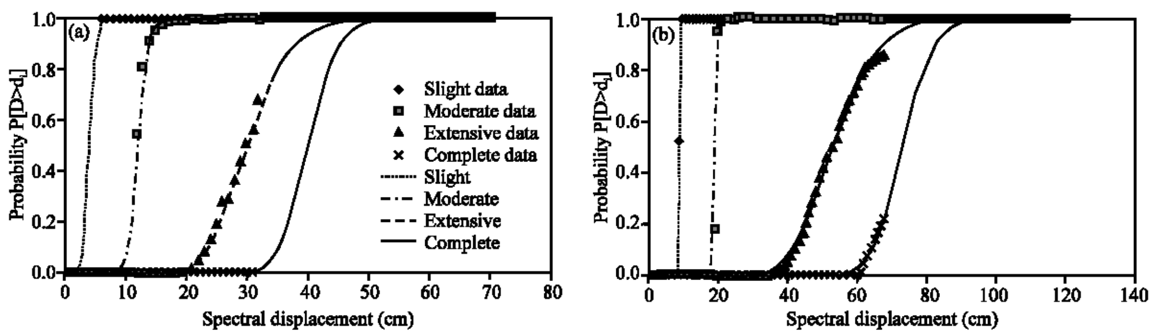

Fig. 13: Fragility function result of simplified method (a) High code and (b) Moderate code

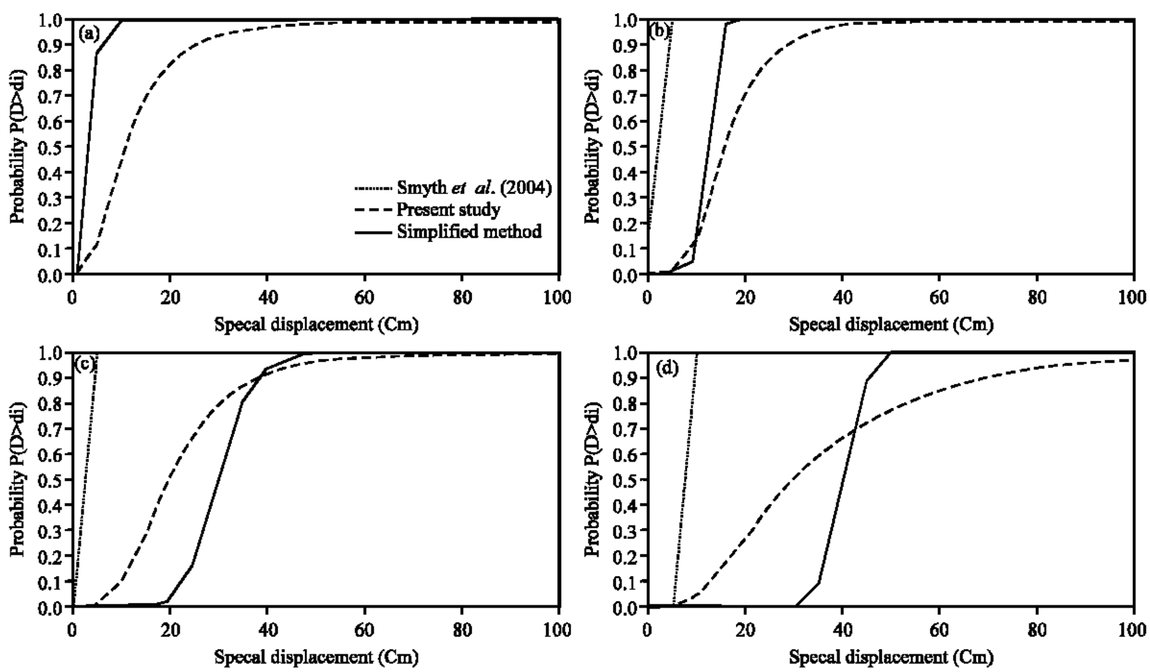

Fig. 14: Comparison of fragility functions for moderate code steel frame structure (a) Slight damage state, (b) Moderate damage state, (c) Extensive damage state and (d) Complete damage state

Table 5: Parameters of fragility functions estimated from simplified procedure

	Slight		Moderate		Extensive		Complete	
Code design level	SD_m (cm)	β	SD_m (cm)	β	SD_m (cm)	β	SD_m (cm)	β
Moderate code	4	0.20	12	0.11	30	0.185	40	0.1
High code	10	0.02	19	0.02	53	0.200	73	0.1

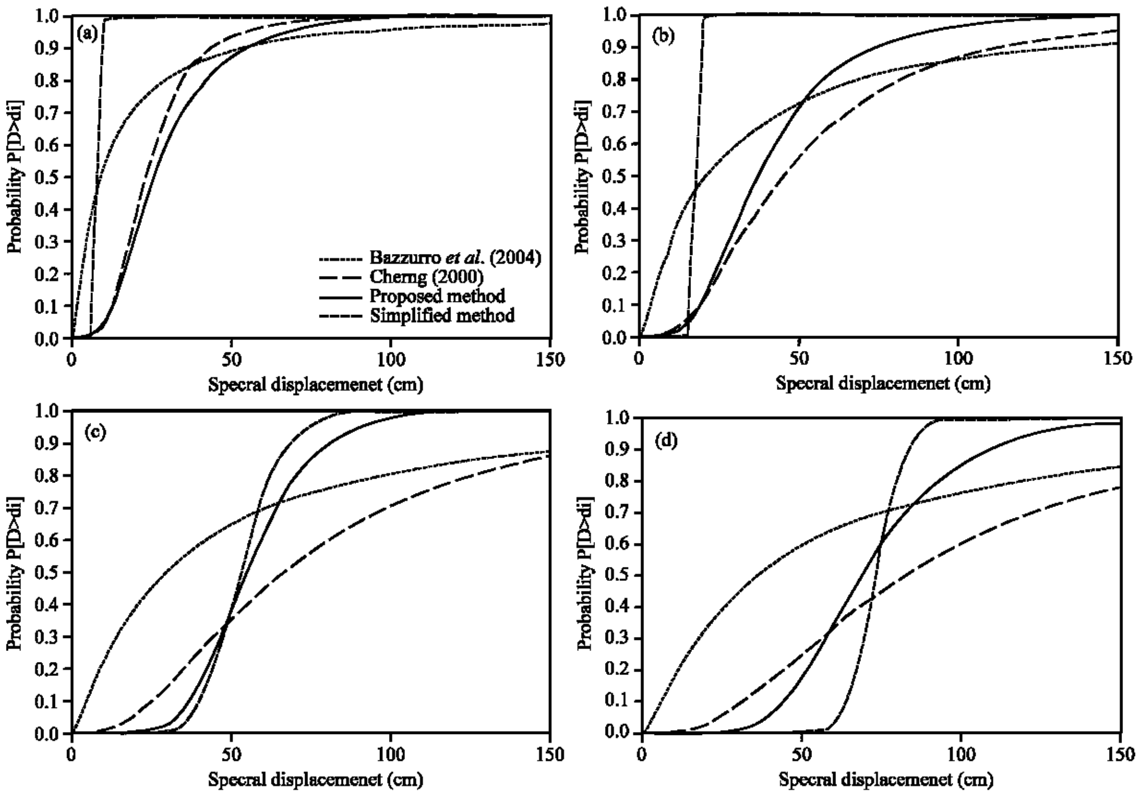

Fig. 15: Comparison of fragility functions for high code steel frame structure (a) Slight damage state, (b) Moderate damage state, (c) Extensive damage state and (d) Complete damage state

$$\beta_{sd} = \ln(x_{16\%}/x_{50\%})/\Phi^{-1}(0.16) = \ln(x_{84\%}/x_{50\%})/\Phi^{-1}(0.84) \quad (8)$$

Fragility value and functions are shown in Fig. 13. The parameters of fragility function are given in Table 5.

Validation: In this study, full and simplified methods for seismic fragility function development of structures are introduced. In addition, application of the method in development of non-structural governing damages is shown and effect of damage threshold uncertainty on the fragility dispersion is estimated.

The result of full and simplified method for high and medium code design frames are compared with fragility of ductile low-rise steel frames developed by Bazzurro *et al.* (2004) and Cherng (2000) and semi-ductile low-rise steel frames developed by Smyth *et al.* (2004) shown in Fig. 14 and 15. It can be observed that in the first place, the results of full and simplified method are very close in the case of extensive and complete damage states and in the second place, the results of the method are almost comparable with the results of previous studies.

CONCLUSION

Development of structure-specific fragility function is the key elements of accurate risk assessment. In this paper, full and simplified methods for seismic fragility function development of structures are introduced. In addition, application of the method in development of non-structural governing damages is shown and effect of damage threshold uncertainty on fragility dispersion is estimated. It is observed that, the results of the proposed methods are almost comparable with the previous studies and the despite of current assumptions, effect of uncertainty of damage state on the deviation of fragility function in the lower intensity of ground motion is high which gradually decreases. This finding shows that current assumptions about constant uncertainty of fragility function might be correct and future investigation in this field is required.

REFERENCES

Aslani, H. and E. Miranda, 2004. Optimization of response simulation for loss estimation using peer's methodology. In: Proceeding of the 13th World Conference on Earthquake Engineering, Vancouver, Canada, Paper No. 1066.

ATC, 1985. Earthquake damage evaluation data for California. American Technology Council Report No. 13.

Bazzurro, P., C.A. Cornell, C. Menun, N. Luco and M. Motahari, 2004. Advanced Seismic Assessment Guidelines. Report for Pacific Gas and Electric/PEER Lifelines Program, Task, pp: 507.

Cherng, R.H., 2000. Preliminary study on the fragility curves for steel structures in taipei. J. Earthquake Eng. Eng. Seismol., 3 (1): 35-42.

Dimova, S.L. and K. Hirata, 2000. Simplified seismic fragility analysis of structures with two types of friction devices. J. Earthquake Eng. Struct. Dyn., 29 (8): 1153-1175.

FEMA-356, 2000. Prestandard and commentary for the seismic rehabilitation of buildings. Federal Emergency Management Agency (FEMA), Doc. No. 356.

Jalayer, F., 2003. Direct probabilistic seismic analysis: Implementing non-linear dynamic assessments. Ph.D Thesis, Stanford University, California.

Hazus, 1999. Earthquake loss estimation methodology-technical manual. Federal Emergency Management Agency and National Institute of Building Science.

Hwang, H.H.M. and J.W. Huo, 1994. Generation of hazard-consistent fragility curves. J. Soil Dyn. Earthquake Eng., 13 (5): 345-354.

Karim, K.R. and F. Yamazaki, 2001. Effect of earthquake ground motions on fragility curves of highway bridge piers based on numerical simulation. J. Earthquake Eng. Struct. Dyn., 30 (12): 1839-1856.

Karim, K.R. and F. Yamazaki, 2003. A simplified method of constructing fragility curves for highway bridges. J. Earthquake Eng. Struct. Dyn., 32 (10): 1603-1626.

Kinali, K. and B.R. Ellingwood, 2007. Seismic fragility assessment of steel frames for consequence-based engineering: A case study for memphis. TN. J. Eng. Struct., 29 (6): 1115-1127.

Kwon, O.S. and A. Elnashai, 2006. The effect of material and ground motion uncertainty on the seismic vulnerability curves of RC structures. J. Eng. Struct., 28 (2): 289-303.

OpenSees, 2006. Open system for earthquake engineering simulation. Free Software Downloaded from http://opensees.berkeley.edu/index.php.

O'Rourke, M.J. and P. So, 2000. Seismic fragility function for on-grade steel tanks. J. Earthquake Spectra, 16 (4): 1167-1183.

PEER, 2007. Online Strong Motion Database. Pacific Earthquake Engineering Research Center. http://peer.berkeley.edu/smcat/.

Porter, K.A., 2000. Assembly-based vulnerability of buildings and its use in seismic performance evaluation and risk-management decision-making. Ph.D Thesis, Stanford University, California.

Porter, K., R. Kennedy and R. Bachman, 2007. Derivation and use of fragility functions in performance-based earthquake engineering. J. Earthquake Spectra, 22 (2): 471-489.

Sabbetta, F., A. Goretti and A. Lucantoni, 1998. Empirical fragility functions from damage surveys and estimated strong ground motion. In: Proceeding of the 11th European Conference on Earthquake Engineering, Paris.

Sarabandari, P., D. Pachakis, S. King and A.S. Kiremidjian, 2004. Empirical fragility functions from recent earthquakes. In: Proceedings of the 13th World Conference on Earthquake Engineering, Vancouver, Canada Paper No. 1211.

Shinozoka, M., M.Q. Feng, J. Lee and T. Naganuma, 2000a. Statically analysis of fragility functions. J. Eng. Mech. ASCE., 126 (12): 1224-1231.

Shinozoka, M., M.Q. Feng, H.K. Kim and S.H. Kim, 2000b. Nonlinear static procedure for fragility function development. J. Eng. Mech. ASCE., 126 (12): 1287-1295.

Singhal, A. and A.S. Kiremidjian, 1996. Method for probabilistic evaluation of seismic structural damage. J. Struct. Eng. ASCE., 122 (12): 1459-1467.

Smyth, A.W., G. Deodatis, G. Franco, Y. He and T. Gurvich, 2004. Evaluating earthquake retrofitting measures for schools: A demonstration of cost-benefit analysis. Columbia University, New York.

Vamvatsikos, D. and C.A. Cornell, 2005. Direct estimation of seismic demand and capacity of multi degree-of-freedom systems through incremental dynamic analysis of single degree of freedom approximation. J. Struct. Eng., 131 (4): 589-599.

Wen, Y.K., B.R. Ellingwood, D. Veneziano and J. Bracci, 2003. Uncertainty modeling in earthquake engineering. MAE Center Project, Report FD-2.